THE JOURNAL OF PHYSICAL CHEMISTRY B

pubs.acs.org/JPCB Article

Aggregation-Induced Intersystem Crossing: Rational Design for Phosphorescence Manipulation

Published as part of The Journal of Physical Chemistry virtual special issue "Peter J. Rossky Festschrift".

Jinxiao Zhang, Shaul Mukamel,* and Jun Jiang*

Cite This: *J. Phys. Chem. B* 2020, 124, 2238−2244 Read Online

ABSTRACT: Phosphorescence of organic molecules has drawn extensive attention due to its potential applications in energy and life science. However, typically intersystem crossing (ISC) in organic molecules is slow due to the small spin−orbit couplings (SOC) and large energy gaps ($\Delta E_{S\text{-}T}$) between different multiplicities. Molecular aggregation offers a practical strategy to manipulate phosphorescent characteristics. In this work, the impact of aggregation on the luminescence properties of π-conjugated benzophenone luminophore 1-dibenzo[b,d]thiophen-2-yl(phenyl)methanone (BDBT) are investigated theoretically using density functional theory (DFT) and time-dependent DFT. Molecular aggregation results in substantial energy splitting and variation of SOC, eventually changing the ISC rate. This is known as the "aggregation-induced intersystem crossing" (AI-ISC) mechanism. Different types of electron donating and withdrawing functional groups are further introduced into BDBT molecular system to tailor the phosphorescent efficiency. We find that functional groups can influence the SOC and energy gaps and further manipulate the phosphorescence efficiency. Molecular systems with donating functional groups have faster ISC rates, and dimers exhibit the best electronic luminescence due to the relatively large SOC and small $\Delta E_{S\text{-}T}$. The AI-ISC mechanism accompanied by group functionalization provides a practical platform for phosphorescence enhancement.

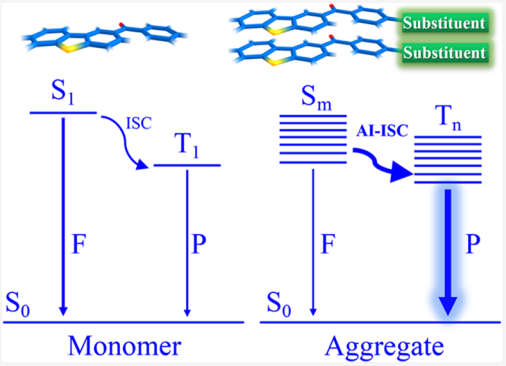

1. INTRODUCTION

Luminescence (fluorescence and phosphorescence) is a useful tool for molecular material applications, including organic light-emitting diodes (OLEDs), sensors, bioimaging, and organic photovoltaic cells.[1−6] Conventional fluorescent devices possess inevitable drawbacks stemming from a limited 25% quantum yield due to the singlet−triplet branching ratio and short nanosecond lifetime.[7] Phosphorescent materials have an advantage, because their quantum yield can reach 75%, and lifetimes are much longer.[8] Pure organic phosphorescent materials have witnessed significant breakthroughs due to their low cost, environmental friendliness, inherent feasible versatility, and good processability compared with inorganics and organometallics.[9−14] However, achieving sufficient intersystem crossing (ISC) remains a major challenge for designing highly efficient phosphorescence.[15,16]

This work focuses on the design of pure organic molecules with high ISC yield. Two strategies are commonly used to facilitate ISC. The ISC rate, $k_{ISC} \propto |\langle T_i|H_{SO}|S_1\rangle|^2/(\Delta E_{S\text{-}T})^2$,[17,18] can be enhanced either by a large $\langle T_i|H_{SO}|S_1\rangle$ or by a small $\Delta E_{S\text{-}T}$. Here $\langle T_i|H_{SO}|S_1\rangle$ and $\Delta E_{S\text{-}T}$ are the spin−orbit couplings (SOC) and energy gap between the lowest singlet excited state and the adjacent triplet excited state, respectively. In pure organic systems ISC has been usually increased by lowering $\Delta E_{S\text{-}T}$ even when the SOC is weak.[19] An alternative approach to an exhaustive search for molecular candidates with small singlet−triplet gaps is to reduce $\Delta E_{S\text{-}T}$ by aggregation. Aggregation is common in π-conjugated systems. However, most planar π-extended aggregates suffer from emission quenching, known as "aggregation caused quenching" (ACQ).[20] Tang et al. coined the term "aggregation induce emission" (AIE) in 2001, and various types of AIE materials have been identified since then.[21] The enhancement of phosphorescence by molecular packing in π-conjugated systems has been reported as well.[22−25]

According to Kasha's rules (Figure 1a), excited energy levels undergo an energy splitting due to excitonic coupling upon aggregation.[26] This will cause the emergence of new energy levels, eventually creating a band structure. As a result, new channels for the transitions between singlet and triplet excited states become available, and energy gaps will be narrowed, eventually enhancing the intersystem crossing rate. Recent

Received: January 23, 2020
Revised: February 24, 2020
Published: February 25, 2020

https://dx.doi.org/10.1021/acs.jpcb.0c00654
J. Phys. Chem. B 2020, 124, 2238−2244

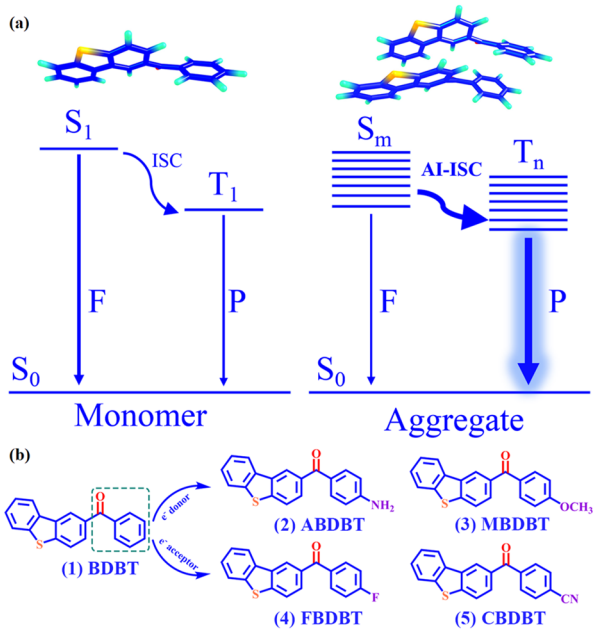

Figure 1. (a) Schematic diagram of AI-ISC. F and P denote fluorescence and phosphorescence, respectively. ISC represents the intersystem crossing from singlet to triplet excited states. The thickness of arrows reflects the strength of promoted ISC or emission. (b) Structures of the organic molecules studied in this work. The top and the bottom rows are the molecular derivatives obtained by incorporating electron donating and withdrawing functional groups into the BDBT molecule, respectively.

advances reveal that high-lying excited states can contribute to phosphorescence.[19,27,28] We anticipate the "aggregation induced intersystem crossing" (AI-ISC) mechanism to open new avenues in the search for candidates with efficient phosphorescence. Molecular aggregation of certain molecules can modulate SOCs and energy gaps and further manipulate ISC rates. Dimers and aggregates with donating functional groups exhibit faster ISC compared with other molecules due to their relatively large SOC and small $\Delta E_{S\text{-}T}$.

Benzophenone and its derivatives (Figure 1b) are short-lived luminophores widely investigated for decades due to their efficient ISC.[29,30] The enhanced ISC in these compounds can be ascribed to their hybrid singlet−triplet transition electronic configuration containing both n and π orbitals, according to El-Sayed's rules.[31] Dibenzo[b,d]thiophen-2-yl(4-fluorophenyl)-methadone (FBDBT), a derivative of benzophenone, shows phosphorescence.[32] Molecular aggregation strongly affects the luminescent properties, while the aggregation behavior and the inherent mechanism in FBDBT remain unknown. The incorporation of a functional group is another favorable strategy to modulate the phosphorescence. In this paper we manipulate molecular aggregation and the functional groups of FBDBT to tune the ISC efficiencies.

With the FBDBT prototype, 1-dibenzo[b,d]thiophen-2-yl(phenyl)methanone (BDBT, 1), we performed density functional theory (DFT) and time-dependent (TD) DFT calculations on its isolated and aggregated forms to explore how aggregation influences its luminescence properties. Functional groups are incorporated as well to modulate SOC and $\Delta E_{S\text{-}T}$. By introducing different electron donating (NH_2−, CH_3O−) and withdrawing (F−, CN−) functional groups into BDBT, we obtained four types of phosphors, namely, dibenzo[b,d]thiophen-2-yl(4-aminophenyl)methadone (ABDBT, 2), dibenzo[b,d]thiophen-2-yl(4-methoxyphenyl)-methadone (MBDBT, 3), FBDBT (4), and dibenzo[b,d]-thiophen-2-yl(4-cyanidephenyl)methadone (CBDBT, 5) as shown in Figure 1b. Our simulated results support the AI-ISC mechanism.

2. COMPUTATIONAL DETAILS

All calculations including geometry optimizations of ground states and excited-state TD-DFT properties were performed with the ADF 2017 program package.[33−35] We employed the B3LYP hybrid exchange-correlation functional, Grimme' D3 dispersion correction term with Becke-Johnson damping parameters (DFT-D3-BJ), and a Slater-type DZP basis set to describe all the molecular structures.[36] DFT-D3-BJ is able to describe the van der Waals interaction, which is crucial in a molecular aggregation process. Statistical average of orbital potentials (SAOP) that can reproduce excitation energies was adopted in the TD-DFT calculations.[37−40] To model the phosphorescence, it is necessary to consider SOC between different multiplicities. Taking the scalar relativistic effect as a perturbation is a reasonable approximation for weak SOC.[41,42] An SAOP model and pSOC-TD-DFT were employed to achieve better excitation properties. Solvent effects of cyclo-hexane were incorporated by the COSMO continuum model in all the calculations described below.

3. RESULTS AND DISCUSSION

BDBT is a π-conjugated derivative consisting of an electron-donating dibenzothiophene and electron-withdrawing benzo-phenone moieties. As can be seen in Figure 2a, both optimized BDBT monomer and aggregates have twisted donor-accept (D−A) structures with similar dihedral angles, and the aggregates exhibit slipped $\pi-\pi$ stacking structures with intermolecular distances of 3.3−3.5 Å due to the van der Waals interaction. We first performed a highest occupied molecular orbital (HOMO)/lowest unoccupied molecular orbital (LUMO) simulation to investigate the nature of the excitations in BDBT. All the HOMOs of BDBT systems are located at the dibenzothiophene moieties, while the LUMOs are centered on the benzophenone moieties, indicating a charge-transfer (CT) character as a result of the D−A model and steric hindrance. The spatial separation of the HOMO and LUMO increases the electron exchange energy and further reduces $\Delta E_{S\text{-}T}$ according to its exponential dependence on the HOMO−LOMO distance. From Figure S5 we see that the system undergoes a sharp decrease of the HOMO−LUMO gap from 2.70 eV in the monomer to 2.40 eV in the tetramer. This will be more favorable for light absorption, since $S_0 \rightarrow S_1$ excitations in all the molecules are dominated by the HOMO → LUMO transition. Additionally, the photoabsorption spectra extend to longer wavelengths in the process of aggregation triggered by the reduction of singlet excited energies (Figure S6a). The oscillator strength and the transition dipole moment of the lowest singlet excited state are the cause of fluorescence emission upon aggregation, resulting in the suppression of fluorescence as illustrated in Figure 2b.

The energy gaps and SOCs are the two dominating factors of the ISC rates. In the course of aggregation, the excited energy levels split, and eventually a band is created as illustrated in Figure 2c. The energy splitting provides new ISC

https://dx.doi.org/10.1021/acs.jpcb.0c00654
J. Phys. Chem. B 2020, 124, 2238−2244

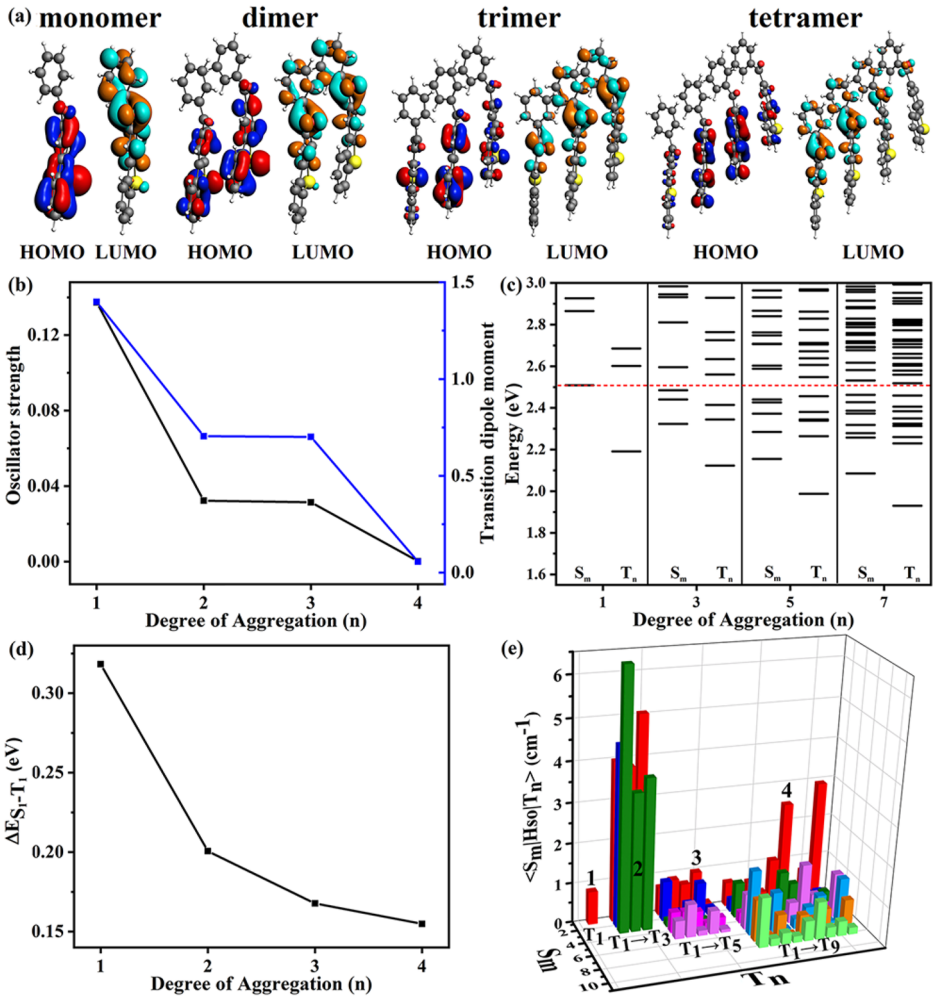

Figure 2. (a) The calculated HOMO and LUMO of model compounds. (b) The calculated oscillator strength and the transition dipole moment of the lowest singlet excited state. (c) The simulated band like excited electronic energy levels. (d) The energy gaps between the lowest singlet and the lowest triplet excited states. (e) The SOCs of BDBT monomer and aggregates. 1, 2, 3, and 4 denote monomer, dimer, trimer, and tetramer, respectively.

channels between the singlet and triplet excited states and narrows the corresponding energy gaps. However, the SOCs of ISC channels show a maximum instead of a monotonic increase with aggregation. Table 1 lists the ISC rates of the channels below the reference red dashed line in Figure 2c. The channel between the lowest singlet and the lowest triplet excited state ($S_1 \rightarrow T_1$) dominates the ISC in BDBT. $\Delta E_{S1\text{-}T1}$ exhibits a sharp decline with aggregation, while the corresponding SOC shows a rise-fall feature. Moreover, high-lying excited states in aggregates also have nontrivial ISC rates, which further promotes the overall ISC rate. Consequently, the overall ISC rates in aggregates increases compared to the monomer, and the dimer has the highest overall ISC rate. The energy gaps, SOCs, and ISC rates of the dominating ISC channels in BDBT molecular system are also calculated with a more sophisticated functional (M06-2X) as shown in Table S5. The ISC rates calculated with M06-2X undergo a rise-fall routine, and dimer holds the fastest ISC rate, which are consistent with our SAOP results. The AI-ISC mechanism can be used to manipulate ISC by balancing the energy gaps and SOCs and further show strong phosphorescence.

To improve the phosphorescent efficiency of BDBT, we investigated a series of derivatives that incorporate electron

Table 1. ISC Rates of BDBT Molecular Systems[a]

	k_{ISC}	S_1	S_2	S_3	S_4	S_5
$(BDBT)_1$	T_1	6.83				
	T_1	395.4	200.1	314.7		
$(BDBT)_2$	T_2		256.6	602.3		
	T_3		6634	2874		
	T_1	17.73	11.44	0.18	1.42	1.00
	T_2		84.04	0.13	9.69	22.25
$(BDBT)_3$	T_3			23.91	27.11	1.60
	T_4			4.00	2.48	37.94
	T_5				24.36	1.70
	T_1	15.40	0.91	6.37	0.50	4.05
	T_2		53.91	1.90	0.29	2.10
$(BDBT)_4$	T_3			109.7	0.15	22.00
	T_4				3.05	6.48
	T_5					114.2

[a]From top to bottom: the calculated ISC rates of the channels below the reference red dashed line in Figure 2c of monomer, dimer, trimer, and tetramer of BDBT. The ISC rates of major channels of isolated/aggregated molecules are in the S_1 column. Note that ISC rates of those channels higher than $S_5 \rightarrow T_5$ in $(BDBT)_4$ can be found in Table S4.

https://dx.doi.org/10.1021/acs.jpcb.0c00654
J. Phys. Chem. B 2020, 124, 2238−2244

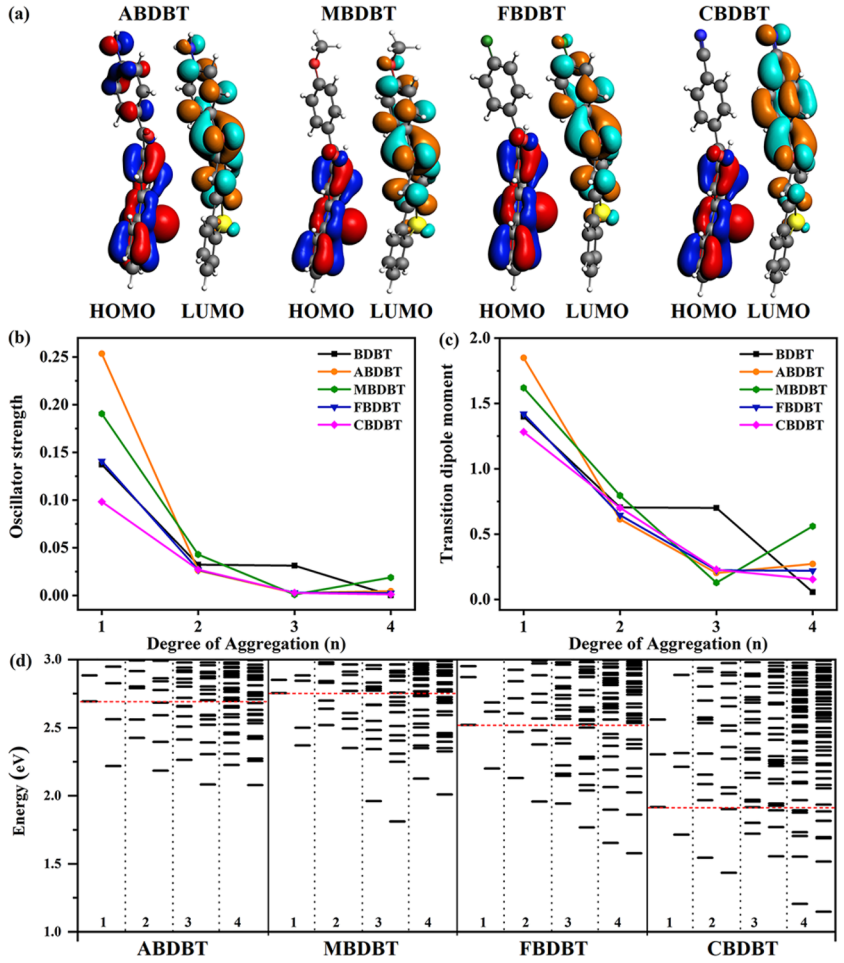

Figure 3. (a) The simulated HOMOs and LUMOs of isolated molecules studied in this work. The HOMOs and LUMOs of aggregates can be found in Figures S1−S4. (b) The calculated emission oscillator strengths and (c) the transition dipole moments from the S_1 to S_0 transition, which produces fluorescence. (d) The calculated singlet and triplet excited energy levels of ABDBT, MBDBT, FBDBT, and CBDBT.

donating ($-OCH_3$, $-NH_2$) and withdrawing (−F, −CN) functional groups into BDBT denoted ABDBT, MBDBT, FBDBT, and CBDBT, respectively (Figure 1b). We then studied the AI-ISC mechanism and the relationship between the cooperating functional groups and electronic structures. All the optimized molecules display distorted D−A conformations, and the optimized aggregates share similar off-plane $\pi-\pi$ stacking structures with intermolecular distances of 3.3−3.5 Å as shown in Figures S1−S4. All molecules exhibit a separation of HOMO and LUMO, reflecting a typical charge transfer character. The HOMO−LUMO overlaps in ABDBT and MBDBT are larger compared to those of FBDBT and CBDBT, which can be ascribed to the electron-donating feature of the $-NH_2$ and $-OCH_3$ substituents. Figure S5 reveals that the HOMO−LUMO gaps are reduced during the aggregation process in all five systems. Additionally, the photoabsorption spectra displayed in Figure S6 generally show red shift during the process of aggregation, which will increase the light utilization. The oscillator strengths and transition dipole moments are examined to further understand the optical properties. Both decrease with aggregation in all the systems as revealed in Figure 3b,c. This should suppress singlet emission and populate the triplet manifold.

Similarly, in the excited energy levels from Figure 3d, all molecules show the emergence of many energy levels between different multiplicities during the aggregation process. Consequently, the singlet−triplet energy gaps decrease, and additional ISC channels become available. The energy gaps between the lowest singlet and the lowest triplet excited states are lowered upon aggregation, as depicted in Figure 4a. We also analyze the energy gaps of the foremost ISC channels in Figure 4b, since $S_1 \rightarrow T_1$ is not always the dominant channel due to the energy splitting. The energy gaps of the dominating ISC channels do not always decrease with aggregation, especially for electron-donating molecular systems. Figure 4c shows the lower-lying ISC channels of the four molecular systems. To sharpen the contrast, we only list the $S_1 \rightarrow T_n$ channels in monomers and channels not higher than $S_2 \rightarrow T_n$ in aggregates. Additional information on excited energies, SOCs, and ISC rates is given in Tables S2−S19. Molecular systems with electron-donating substituents usually have larger SOCs, and dimers typically show relatively large SOCs. We also compared the foremost ISC channels of the five molecular systems. The dominating ISC channels of ABDBT and MBDBT possess larger SOCs and relatively small energy gaps, which promotes the ISC rates as displayed in Figure 4d and Table S19. Dimers show the fastest ISC rates in all five systems. It is worth noting that the phosphorescence lifetimes become longer with aggregation (Table 2). Donating functional groups including amino and methyl moieties combined with molecular aggregation can facilitate the overall ISC rate and promote the photoluminescence. The AI-ISC mechanism

https://dx.doi.org/10.1021/acs.jpcb.0c00654
J. Phys. Chem. B 2020, 124, 2238−2244

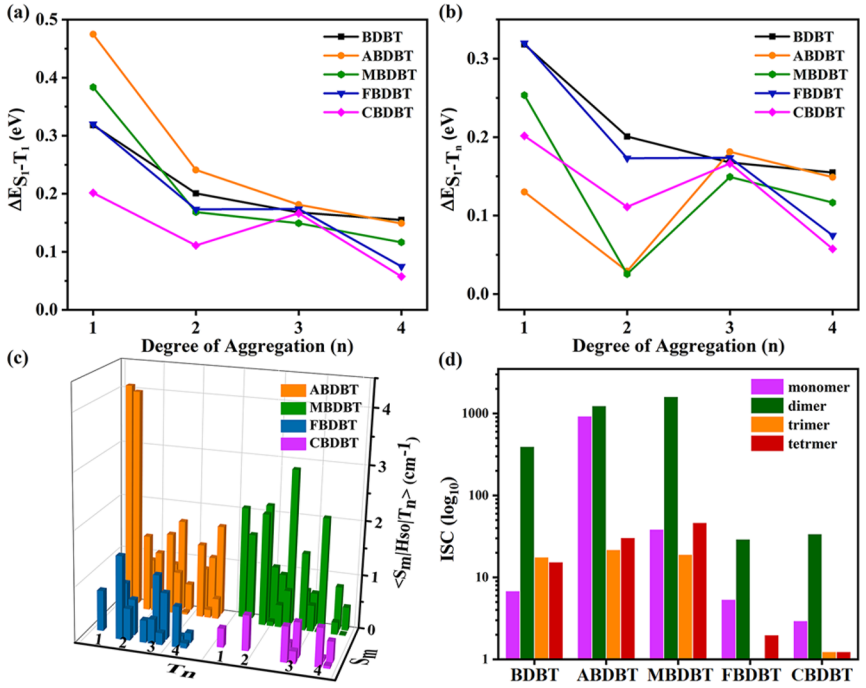

Figure 4. (a) Calculated energy gaps of the lowest singlet and triplet excited states. (b) The calculated energy gaps of the lowest singlet and the adjacent triplet excited states. (c) The SOCs of the important lower-lying ISC channels of the four molecular systems. 1, 2, 3, and 4 denote monomer, dimer, trimer, and tetramer, respectively. For monomer, we only list $S_1 \rightarrow T_n$ channels. For aggregates, we only list the channels not higher than their own $S_2 \rightarrow T_m$ channels and $S_1 \rightarrow T_m$ channels of their corresponding monomers. More details can be found in Tables S2−S19. (d) ISC rates of the dominated channels in monomer and aggregates. The ISC values are plotted in $\log_{10}$ format, and the absolute ISC values can be attained in Table S19.

Table 2. Phosphorescent Lifetimes of the Five Molecular Systems

lifetime/s	BDBT	ABDBT	MBDBT	FBDBT	CBDBT
monomer	0.014	0.003	0.002	0.019	0.068
dimer	0.025	0.014	0.010	0.063	0.131
trimer	0.118	0.036	0.425	0.164	0.417
tetramer	0.336	0.092	0.118	1.402	1.621

in combination with substituent modulations can be a feasible approach for us to manipulate phosphorescence and hence increase the energy utilization.

4. CONCLUSIONS

The aggregation-induced intersystem crossing mechanism was studied, and substituent effects were employed to manipulate the ISC efficiency to pursue highly efficient phosphorescence by a series of DFT/TD-DFT calculations. BDBT was first chosen to design aggregates, which exhibited slipped $\pi-\pi$ stacking structures. Appropriate molecular distances in aggregates reduce the oscillator strength and the transition dipole moment of the lowest singlet excited state, which resulted in the suppression of fluorescence and enhancement of the conversion possibility from singlet to triplet manifold. At the same time, the strong intermolecular interactions cause the excited energy splitting and achieve a band like section during the process of aggregation. The new energy levels provide additional ISC channels and narrow the energy gaps between the singlet excited and the adjacent triplet excited states. However, the SOC generally show a rise-fall feature during the process of aggregation. Consequently, BDBT dimer shows faster ISC rate compared with monomer and other aggregates. Four functional groups were introduced into BDBT to tune phosphorescence properties. Molecules with electron-donating substitutes showed larger SOC, and the $\Delta E_{S\text{-}T}$ values were not very large, which eventually led to a superior ISC rate compared with that of withdrawing functional groups. Notably, dimers displayed the best phosphorescence efficiency in all the molecular aggregated systems, since they typically have large SOCs. Therefore, we need to find a balance between SOC and $\Delta E_{S\text{-}T}$ to achieve optimized ISC rates. Aggregation induced by van der Waals interaction possesses a remarkable versatility in molecular design, and therefore it is conceivable that AI-ISC can serve as a complement for AIE. Our results provide a promising platform for developing highly efficient phosphorescence materials.

■ ASSOCIATED CONTENT

Supporting Information

The Supporting Information is available free of charge at https://pubs.acs.org/doi/10.1021/acs.jpcb.0c00654.

HOMO and LUMOs, HOMO−LUMO gaps, photoabsorption spectra, energy levels of singlet and triplet excited states, SOC and ISC rates of all the molecular systems (PDF)

■ AUTHOR INFORMATION

Corresponding Authors

Shaul Mukamel − *Department of Chemistry, Department of Physics and Astronomy, University of California, Irvine, California 92697, United States;* orcid.org/0000-0002-6015-3135; Email: smukamel@uci.edu

Jun Jiang − *Hefei National Laboratory for Physical Sciences at the Microscale, Collaborative Innovation Center of Chemistry*

https://dx.doi.org/10.1021/acs.jpcb.0c00654
J. Phys. Chem. B 2020, 124, 2238−2244

for Energy Materials, CAS Center for Excellence in Nanoscience, School of Chemistry and Materials Science, University of Science and Technology of China, Hefei, Anhui 230026, P. R. China; orcid.org/0000-0002-6116-5605; Email: jiangj1@ustc.edu.cn

Author

Jinxiao Zhang − *Hefei National Laboratory for Physical Sciences at the Microscale, Collaborative Innovation Center of Chemistry for Energy Materials, CAS Center for Excellence in Nanoscience, School of Chemistry and Materials Science, University of Science and Technology of China, Hefei, Anhui 230026, P. R. China*

Complete contact information is available at: https://pubs.acs.org/10.1021/acs.jpcb.0c00654

Author Contributions

The manuscript was written through contributions of all authors. All authors have given approval to the final version of the manuscript.

Notes

The authors declare no competing financial interest.

■ ACKNOWLEDGMENTS

This work was financially supported by MOST (2018YFA0208603) and NSFC (21633006). S.M. was supported by the U.S. Department of Energy, Office of Science, and Basic Energy Sciences under Award No. 60054427. The numerical calculations in this paper were done in the Supercomputing Center of University of Science and Technology of China.

■ REFERENCES

(1) Zhang, K. Y.; Yu, Q.; Wei, H.; Liu, S.; Zhao, Q.; Huang, W. Long-Lived Emissive Probes for Time-Resolved Photoluminescence Bioimaging and Biosensing. *Chem. Rev.* **2018**, *118*, 1770−1839.

(2) Li, K.; Ming Tong, G. S.; Wan, Q.; Cheng, G.; Tong, W. Y.; Ang, W. H.; Kwong, W. L.; Che, C. M. Highly Phosphorescent Platinum(II) Emitters: Photophysics, Materials and Biological Applications. *Chem. Sci.* **2016**, *7*, 1653−1673.

(3) Yen, W. M.; Shionoya, S.; Yamamoto, H. *Practical Applications of Phosphors;* CRC Press: Boca Raton, FL, 2006.

(4) Xiang, H.; Cheng, J.; Ma, X.; Zhou, X.; Chruma, J. J. Near-Infrared Phosphorescence: Materials and Applications. *Chem. Soc. Rev.* **2013**, *42*, 6128−6185.

(5) Murphy, L.; Williams, J. A. G. Luminescent Platinum Compounds: From Molecules to OLEDs. In *Molecular Organometallic Materials for Optics;* Bozec, H., Guerchais, V., Eds.; Springer Berlin Heidelberg: Berlin, Germany, 2010; Vol. *28*, pp 75−111.

(6) Valeur, B.; Berberan-Santos, M. N. A Brief History of Fluorescence and Phosphorescence Before the Emergence of Quantum Theory. *J. Chem. Educ.* **2011**, *88*, 731−738.

(7) Köhler, A.; Wilson, J. S.; Friend, R. H. Fluorescence and Phosphorescence in Organic Materials. *Adv. Mater.* **2002**, *14*, 701−707.

(8) Becker, R. S. *Theory and Interpretation of Fluorescence and Phosphorescence;* Wiley Interscience: New York, 1969.

(9) Wang, S.; Yuan, W. Z.; Zhang, Y. Pure Organic Luminogens with Room Temperature Phosphorescence. In *Aggregation-Induced Emission: Materials and Applications;* American Chemical Society: Washington, DC, 2016; Vol. *2*, pp 1−26.

(10) Mukherjee, S.; Thilagar, P. Recent Advances in Purely Organic Phosphorescent Materials. *Chem. Commun.* **2015**, *51*, 10988−11003.

(11) Zhao, W.; Cheung, T. S.; Jiang, N.; Huang, W.; Lam, J. W. Y.; Zhang, X.; He, Z.; Tang, B. Z. Boosting the Efficiency of Organic Persistent Room-Temperature Phosphorescence by Intramolecular Triplet-Triplet Energy Transfer. *Nat. Commun.* **2019**, *10*, 1595.

(12) Kenry; Chen, C.; Liu, B. Enhancing the Performance of Pure Organic Room-Temperature Phosphorescent Luminophores. *Nat. Commun.* **2019**, *10*, 2111.

(13) Zhang, X.; Du, L.; Zhao, W.; Zhao, Z.; Xiong, Y.; He, X.; Gao, P. F.; Alam, P.; Wang, C.; Li, Z.; et al. Ultralong UV/Mechano-Excited Room Temperature Phosphorescence from Purely Organic Cluster Excitons. *Nat. Commun.* **2019**, *10*, 5161.

(14) Shoji, Y.; Ikabata, Y.; Wang, Q.; Nemoto, D.; Sakamoto, A.; Tanaka, N.; Seino, J.; Nakai, H.; Fukushima, T. Unveiling a New Aspect of Simple Arylboronic Esters: Long-Lived Room-Temperature Phosphorescence from Heavy-Atom-Free Molecules. *J. Am. Chem. Soc.* **2017**, *139*, 2728−2733.

(15) Kwon, M. S.; Yu, Y.; Coburn, C.; Phillips, A. W.; Chung, K.; Shanker, A.; Jung, J.; Kim, G.; Pipe, K.; Forrest, S. R.; et al. Suppressing Molecular Motions for Enhanced Room-Temperature Phosphorescence of Metal-Free Organic Materials. *Nat. Commun.* **2015**, *6*, 8947.

(16) Deng, Y.; Zhao, D.; Chen, X.; Wang, F.; Song, H.; Shen, D. Long Lifetime Pure Organic Phosphorescence Based on Water Soluble Carbon Dots. *Chem. Commun.* **2013**, *49*, 5751−5753.

(17) Chen, Y. L.; Li, S. W.; Chi, Y.; Cheng, Y. M.; Pu, S. C.; Yeh, Y. S.; Chou, P. T. Switching Luminescent Properties in Osmium-Based *β*-Diketonate Complexes. *ChemPhysChem* **2005**, *6*, 2012−2017.

(18) Englman, R.; Jortner, J. The Energy Gap Law for Radiationless Transitions in Large Molecules. *Mol. Phys.* **1970**, *18*, 145−164.

(19) Marian, C. M. Spin-Orbit Coupling and Intersystem Crossing in Molecules. *WIREs Comput. Mol. Sci.* **2012**, *2*, 187−203.

(20) Hong, Y.; Lam, J. W. Y.; Tang, B. Z. Aggregation-Induced Emission. *Chem. Soc. Rev.* **2011**, *40*, 5361−5388.

(21) Luo, J.; Xie, Z.; Lam, J. W.; Cheng, L.; Chen, H.; Qiu, C.; Kwok, H. S.; Zhan, X.; Liu, Y.; Zhu, D.; et al. Aggregation-Induced Emission of 1-Methyl-1,2,3,4,5-Pentaphenylsilole. *Chem. Commun.* **2001**, 1740−1741.

(22) Yang, L.; Wang, X.; Zhang, G.; Chen, X.; Zhang, G.; Jiang, J. Aggregation-Induced Intersystem Crossing: A Novel Strategy for Efficient Molecular Phosphorescence. *Nanoscale* **2016**, *8*, 17422−17426.

(23) Xie, Y.; Ge, Y.; Peng, Q.; Li, C.; Li, Q.; Li, Z. How the Molecular Packing Affects the Room Temperature Phosphorescence in Pure Organic Compounds: Ingenious Molecular Design, Detailed Crystal Analysis, and Rational Theoretical Calculations. *Adv. Mater.* **2017**, *29*, 1606829.

(24) Yang, J.; Zhen, X.; Wang, B.; Gao, X.; Ren, Z.; Wang, J.; Xie, Y.; Li, J.; Peng, Q.; Pu, K.; et al. The Influence of the Molecular Packing on the Room Temperature Phosphorescence of Purely Organic Luminogens. *Nat. Commun.* **2018**, *9*, 840.

(25) Wang, X. F.; Xiao, H.; Chen, P. Z.; Yang, Q. Z.; Chen, B.; Tung, C. H.; Chen, Y. Z.; Wu, L. Z. Pure Organic Room Temperature Phosphorescence from Excited Dimers in Self-Assembled Nanoparticles under Visible and Near-Infrared Irradiation in Water. *J. Am. Chem. Soc.* **2019**, *141*, 5045−5050.

(26) Kasha, M.; Rawls, H.; El-Bayoumi, M. A. The Exciton Model in Molecular Spectroscopy. *Pure Appl. Chem.* **1965**, *11*, 371−392.

(27) Itoh, T. Fluorescence and Phosphorescence from Higher Excited States of Organic Molecules. *Chem. Rev.* **2012**, *112*, 4541−4568.

(28) Yu-Tzu Li, E.; Jiang, T. Y.; Chi, Y.; Chou, P. T. Semi-Quantitative Assessment of the Intersystem Crossing Rate: An Extension of the El-Sayed Rule to the Emissive Transition Metal Complexes. *Phys. Chem. Chem. Phys.* **2014**, *16*, 26184−26192.

(29) Kearns, D. R.; Case, W. A. Investigation of Singlet → Triplet Transitions by the Phosphorescence Excitation Method. III. Aromatic Ketones and Aldehydes. *J. Am. Chem. Soc.* **1966**, *88*, 5087−5097.

(30) Lee, S. Y.; Yasuda, T.; Yang, Y. S.; Zhang, Q.; Adachi, C. Luminous Butterflies: Efficient Exciton Harvesting by Benzophenone Derivatives for Full-Color Delayed Fluorescence OLEDs. *Angew. Chem.* **2014**, *126*, 6520−6524.

(31) Shimakura, N.; Fujimura, Y.; Nakajima, T. Theory of Intersystem Crossing in Aromatic Compounds: Extension of the El-Sayed Rule. *Chem. Phys.* **1977**, *19*, 155−163.
(32) Zhao, W.; He, Z.; Lam, J. W. Y.; Peng, Q.; Ma, H.; Shuai, Z.; Bai, G.; Hao, J.; Tang, B. Z. Rational Molecular Design for Achieving Persistent and Efficient Pure Organic Room-Temperature Phosphorescence. *Chem.* **2016**, *1*, 592−602.
(33) Te Velde, G.; Bickelhaupt, F. M.; Baerends, E. J.; Fonseca Guerra, C.; van Gisbergen, S. J. A.; Snijders, J. G.; Ziegler, T. Chemistry with ADF. *J. Comput. Chem.* **2001**, *22*, 931−967.
(34) Fonseca Guerra, C.; Snijders, J. G.; te Velde, G.; Baerends, E. J. Towards an Order-N DFT Method. *Theor. Chem. Acc.* **1998**, *99*, 391−403.
(35) Baerends, E. J.; Ziegler, T.; Autschbach, J.; Bashford, D.; Bérces, A.; Bickelhaupt, F. M.; Bo, C.; Boerrigter, P. M.; Cavallo, L.; Chong, D. P.; et al. *ADF2017, SCM: Theoretical Chemistry;* Vrije Universiteit: Amsterdam, The Netherlands, 2017.
(36) Van Lenthe, E.; Baerends, E. J. Optimized Slater-Type Basis Sets for the Elements 1−118. *J. Comput. Chem.* **2003**, *24*, 1142−1156.
(37) Chong, D. P.; Gritsenko, O. V.; Baerends, E. J. Interpretation of the Kohn-Sham Orbital Energies as Approximate Vertical Ionization Potentials. *J. Chem. Phys.* **2002**, *116*, 1760−1772.
(38) Ricciardi, G.; Rosa, A.; Baerends, E. J. Ground and Excited States of Zinc Phthalocyanine Studied by Density Functional Methods. *J. Phys. Chem. A* **2001**, *105*, 5242−5254.
(39) Barrera, M.; Crivelli, I.; Loeb, B. On the Performance of Ruthenium Dyes in Dye Sensitized Solar Cells: A Free Cluster Approach Based on Theoretical Indexes. *J. Mol. Model.* **2016**, *22*, 118.
(40) Gritsenko, O. V.; Schipper, P. R. T.; Baerends, E. J. Approximation of the Exchange-Correlation Kohn-Sham Potential with a Statistical Average of Different Orbital Model Potentials. *Chem. Phys. Lett.* **1999**, *302*, 199−207.
(41) Wang, F.; Ziegler, T. A Simplified Relativistic Time-Dependent Density-Functional Theory Formalism for the Calculations of Excitation Energies Including Spin-Orbit Coupling Effect. *J. Chem. Phys.* **2005**, *123*, 154102−154112.
(42) Mori, K.; Goumans, T. P.; van Lenthe, E.; Wang, F. Predicting Phosphorescent Lifetimes and Zero-Field Splitting of Organometallic Complexes with Time-Dependent Density Functional Theory Including Spin-Orbit Coupling. *Phys. Chem. Chem. Phys.* **2014**, *16*, 14523−14530.

https://dx.doi.org/10.1021/acs.jpcb.0c00654
J. Phys. Chem. B 2020, 124, 2238−2244